# Imaging of the Porta Hepatis: Spectrum of Disease[1]

Sree Harsha Tirumani, MD
Alampady Krishna Prasad
    Shanbhogue, MD
Raghunandan Vikram,
    MBBS, MRCP, FRCR
Srinivasa R. Prasad, MD
Christine O. Menias, MD[2]

## SA-CME LEARNING OBJECTIVES FOR TEST 2

*After completing this journal-based SA-CME activity, participants will be able to:*

■ Describe the anatomy of the porta hepatis and its adjacent peritoneal reflections.

■ Discuss the wide array of diseases that affect the porta hepatis and its role as a pathway for disease spread.

■ Identify the role of imaging in diagnosis and management of diseases of the porta hepatis.

*See www.rsna.org/education/search/RG*

**TEACHING POINTS**
*See last page*

A wide array of pathologic conditions can arise within the porta hepatis, which encompasses the portal triad (the main portal vein, common hepatic artery, and common bile ducts), lymphatics, nerves, and connective tissue. Major vascular diseases of the portal triad include thrombosis, stenosis, and aneurysm. Portal vein thrombosis can complicate liver cirrhosis and hepatocellular carcinoma and has important therapeutic implications. Hepatic artery thrombosis and stenosis require immediate attention to reduce graft loss in liver transplant recipients. Congenital (eg, choledochal cyst) and acquired (benign and malignant) diseases of the biliary system can manifest as mass lesions in the porta hepatis. Lymphadenopathy can arise from neoplastic and nonneoplastic entities. Uncommon causes of mass lesions arise from nerves (eg, neurofibroma, neurofibrosarcoma) and connective tissue (sarcomas) and are rare. The hepatoduodenal ligament is a peritoneal reflection at the porta hepatis and is an important route for the spread of pancreatic and gastrointestinal cancers. Imaging plays a major role in diagnosis and enables appropriate management. Ultrasonography accurately demonstrates anatomic variations and pathologic conditions and is the initial modality of choice for detection of vascular and biliary lesions. Multidetector computed tomography and magnetic resonance imaging allow characterization and differentiation of various masses in the porta hepatis. Imaging-guided interventions, including embolization and stent placement, also play a key role in disease management.

©RSNA, 2014 • *radiographics.rsna.org*

## Introduction

The complex anatomic architecture of the porta hepatis makes imaging of this region challenging as well as critical. A wide spectrum of neoplastic and nonneoplastic pathologic conditions can occur in the structures that form the porta hepatis (Table 1). Advances in imaging modalities and improved spatial resolution of current imaging techniques have enabled greater accuracy in diagnosing these conditions. We describe the anatomy of the porta hepatis and review the clinical, pathologic, and imaging features of various diseases involving the porta hepatis.

## Radiologic Anatomy

The *porta hepatis*, or hilum of the liver, is a deep, short, transverse fissure that passes across the left posterior aspect of the undersurface of the right lobe of the liver. It separates the caudate lobe and process from the quadrate lobe and meets the left sagittal fossa perpendicularly (1). The porta hepatis transmits the portal triad—formed by the main portal vein, proper hepatic artery, and common hepatic duct—as well as nerves and lymphatics (1). The portal vein, proper hepatic artery, and nerves derived from the left vagal trunk and sympathetic plexus ascend the porta hepatis, whereas the common bile duct and lymphatics descend the porta hepatis. All of these structures are enveloped in the free edge of the lesser omentum or hepatoduodenal ligament, loose areolar tissue, and the fibrous capsule of Glisson. The hepatoduodenal ligament also envelops the gallbladder neck and cystic duct and distally inserts between the first and second portions of the duodenum (Fig 1).

**Teaching Point**

Within the porta hepatis, the common bile duct and proper hepatic artery typically are located anterior to the portal vein, with the common bile duct to the right and the proper hepatic artery to the left (Fig 1). The proper hepatic artery branches into the right and left hepatic arteries, with the right hepatic artery passing between the portal vein and common bile duct. Several variations in this relation can occur, some of which are due to aberrant and accessory hepatic arteries. Lymphatic channels in the hepatoduodenal ligament drain the liver, gallbladder, bile ducts, duodenum, stomach, and pancreas into the paraaortic nodes near the origin of the superior mesenteric artery (2). The nerves that course through the porta hepatis are branches of the left vagus nerve and sympathetic branches of the celiac plexus.

## Imaging Modalities for Evaluation

Ultrasonography (US) is the most widely used, inexpensive, easily available modality for evaluation of the porta hepatis (Table 2). The availability of high-resolution transducers has increased the sensitivity of US for daily practice. Color, spectral, and power Doppler US provide indispensable information about the vascular structures in the porta hepatis. The common hepatic duct is seen on gray-scale US images as a linear tubular structure anterolateral to the portal vein with echogenic walls and an anechoic lumen. The normal portal vein has an anechoic lumen and low-velocity hepatopedal venous flow with characteristic phasicity. The hepatic artery shows pulsatile high-velocity arterial flow. Advances such as three-dimensional US and US contrast agents

have added a new dimension to US examinations of the porta hepatis. However, the relatively low accuracy and operator dependence of US often necessitate additional investigation with other imaging modalities.

MDCT is the imaging modality of choice for comprehensive evaluation of the porta hepatis (Table 2). Multiphasic image acquisition in the unenhanced, arterial, venous, and delayed phases allows assessment of the dynamic enhancement characteristics of benign and malignant diseases of the porta hepatis. The common bile duct appears at MDCT as a linear fluid-filled structure

**Table 1: Spectrum of Vascular and Nonvascular Diseases of the Porta Hepatis**

| Disease Type and Location |
| --- |
| Vascular |
|   Main portal vein |
|     Thrombosis |
|     Stenosis |
|     Aneurysm |
|     Gas |
|   Common hepatic artery |
|     Thrombosis |
|     Stenosis |
|     Aneurysm |
| Nonvascular |
|   Biliary tree |
|     Cholangiocarcinoma |
|     Intrabiliary metastasis |
|     Benign stricture |
|     Choledochal cyst |
|   Lymphatics, nerves, and connective tissue |
|     Lymph nodes |
|       Benign reactive lymph nodes |
|       Noninfectious inflammatory disease |
|       Infectious disease |
|       Metastasis |
|       Lymphoma |
|       PTLD |
|     Nerves |
|       Schwannoma |
|       Neurofibroma |
|       Neurofibrosarcoma |
|     Connective tissue |
|       Rhabdomyosarcoma |
|       Granulocytic sarcoma |

Note.—Miscellaneous pathologic features include periportal edema, fluid collection, laceration, artifacts, and structures that act as pathways of disease spread. PTLD = posttransplant lymphoproliferative disorder.

**Figure 1.**   Radiologic anatomy of the porta hepatis. **(a)** Anatomic diagram of the inferior surface of the liver (viewed from below) shows the major anatomic relations of the porta hepatis. *CBD* = common bile duct, *CHA* = common hepatic artery, *GB* = gallbladder, *IVC* = inferior vena cava, *MPV* = main portal vein. **(b)** Axial contrast-enhanced CT image shows the relations of the common bile duct (white arrow), common hepatic artery (black arrow), main portal vein (white arrowhead), and inferior vena cava (black arrowhead). **(c)** Anatomic diagram (anterior view, with liver retracted anteriosuperiorly) shows the major ligaments related to the porta hepatis. **(d)** Coronal contrast-enhanced CT image shows the relation of the porta hepatis to the surrounding viscera. The common bile duct (white arrow), common hepatic artery (black arrow), and main portal vein (arrowhead) are transmitted through the porta hepatis.
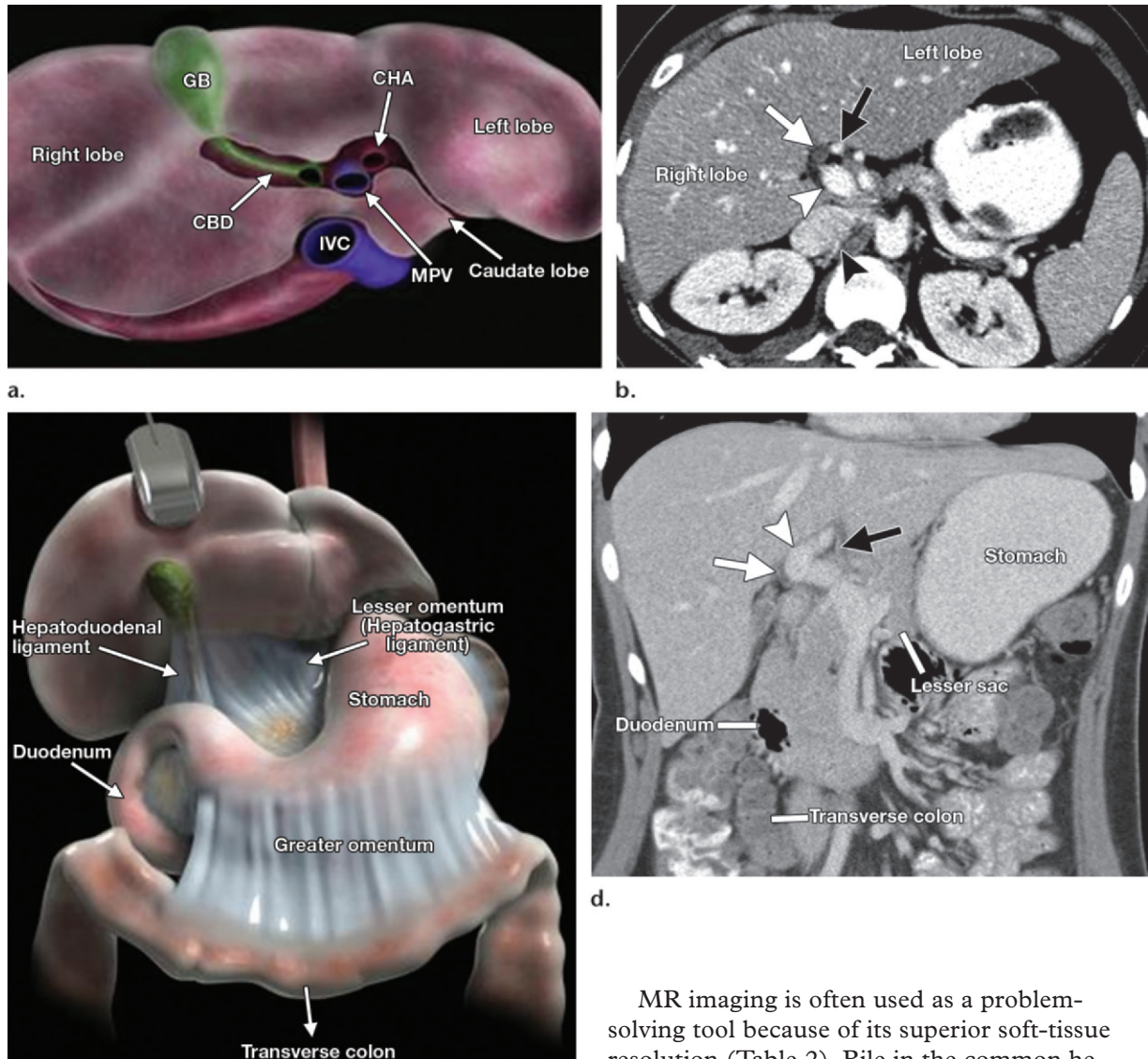


with no perceptible wall. The normal portal vein has a diameter of 11–13 mm and enhances uniformly in the portal venous phase (60–70 seconds after contrast agent administration). The hepatic artery is well demonstrated in the arterial phase (20–25 seconds after contrast agent administration) and with MDCT angiography. Multiplanar reformations and advanced post-processing techniques increase the diagnostic accuracy of MDCT. Exposure to radiation and nephrotoxicity of contrast media are some of the limitations of MDCT.

MR imaging is often used as a problem-solving tool because of its superior soft-tissue resolution (Table 2). Bile in the common hepatic duct gives rise to its high signal intensity on MR images. The portal vein and hepatic artery demonstrate flow voids at routine MR imaging sequences. The newer fast MR imaging sequences allow shorter imaging times with improved image quality. Dynamic imaging after gadolinium-based contrast agent administration and diffusion-weighted imaging can help differentiate benign from malignant tumors. MR cholangiography is the imaging modality of choice for the biliary tree and is preferred over ERCP for initial evaluation. FDG PET/CT is increasingly used to characterize and stage malignant diseases of the porta hepatis, notably cholangiocarcinoma (3).

**Table 2: Utility of Various Modalities for Imaging of the Porta Hepatis**

| Imaging Modality | Utility |
|---|---|
| **US** | |
| Gray-scale imaging: subcostal or intercostal approach | Initial investigation of choice |
| Color and spectral Doppler US | Doppler US allows quantification of flow velocities |
| **MDCT** | |
| Multiphasic acquisition: unenhanced, arterial (20–25 sec), venous (60–70 sec), delayed (1–3 min) phases | Most comprehensive investigation<br>Allows evaluation of most diseases of the porta hepatis |
| Postprocessing techniques: multiplanar reformations, volume rendering | Staging of malignancies |
| MDCT angiography | Demonstrates arterial anatomy |
| **MR imaging** | |
| Multiplanar T1- and T2-weighted images, MRCP, dynamic gadolinium-enhanced imaging, diffusion-weighted imaging | Problem-solving tool<br>Useful for patients with contraindications to CT<br>Evaluation of biliary tree |
| **PET/CT** | |
| FDG used as a tracer to detect metabolic activity | Evaluation of malignancies such as cholangiocarcinoma<br>Combined PET/CT allows better anatomic localization |
| **ERCP** | |
| Endoscopic cannulation of the common bile duct followed by contrast agent injection or interventions such as balloon dilation and stent placement | Diagnosis and treatment of biliary strictures |
| **Conventional angiography** | |
| Percutaneous transarterial or transhepatic cannulation of the hepatic artery or portal vein, respectively | Diagnosis and management of aneurysms or stenosis in the hepatic artery and portal vein |

Note.—CT = computed tomography, ERCP = endoscopic retrograde cholangiopancreatography, FDG = fluorine 18 fluorodeoxyglucose, MDCT = multidetector CT, MR = magnetic resonance, MRCP = MR cholangiopancreatography, PET = positron emission tomography.

## Spectrum of Disease

A broad classification of diseases that affect the porta hepatis includes vascular and nonvascular pathologic conditions. The salient imaging features of diseases encountered in the porta hepatis are summarized in Table 3.

## Vascular Diseases

### Diseases of the Portal Vein

***Portal Vein Thrombosis.***—Thrombosis of the portal vein is seen with various pathologic conditions. Common causes include cirrhosis; cholangitis; pancreatitis; appendicitis; diverticulitis; neoplasms such as hepatocellular carcinoma and pancreatic cancer; hypercoagulable states; and surgeries such as liver transplantation, splenectomy, and portosystemic shunt surgery (4). Bland portal vein thrombosis occurs in 11.2%–15.8% of cases of cirrhosis because of hypertension-related portal venous stasis (5,6) (Fig 2). Hepatocellular carcinoma, by virtue of its portal venous drainage, can invade the portal vein directly, resulting in malig-

nant portal vein thrombosis in up to 44% of cases (6,7). The disease course in portal vein thrombosis depends on the degree of thrombosis, extent of collateralization, and duration of the thrombus. Acute thrombosis can be asymptomatic, can exacerbate preexisting portal hypertension, or can result in variceal bleeding and shock (4). Chronic thrombosis is associated with splenomegaly, gastroesophageal varices, ascites, and chronic gastrointestinal bleeding. *Cavernous transformation of the portal vein* refers to multiple tortuous venous collaterals at the porta hepatis that replace the occluded portal vein; this can occur as early as 20 days after thrombosis (8) (Fig 3).

US depicts acute thrombosis as a dilated portal vein with absence of flow. Acute thrombus can be anechoic, whereas subacute and chronic thrombus is echogenic (9). Color Doppler US allows real-time evaluation of portal venous flow. Evaluation with spectral and power Doppler US is essential to differentiate the sluggish flow seen with severe portal hypertension from portal vein thrombosis. Prominent hepatic artery inflow is an indirect sign of portal vein

**Table 3: Imaging Features of Vascular and Nonvascular Diseases of the Porta Hepatis**

| Location and Disease Type | Imaging Features |
|---|---|
| **Portal vein** | |
| Thrombosis | Absent flow on color Doppler US images, lack of enhancement on MDCT or MR images; in acute thrombosis, echogenic or hyperattenuating thrombus; in chronic thrombosis, cavernous transformation and calcification; in malignant thrombosis, high-signal-intensity thrombus on T2-weighted images, neovascular channels, thrombus contiguous with the primary hepatic tumor, appearance similar to primary neoplasm |
| Stenosis | Focal narrowing of the portal vein and secondary portal hypertension; Doppler US better demonstrates velocity changes: focal aliasing, three- to fourfold velocity gradient across the anastomosis |
| Aneurysm | Focal dilatation of the portal vein (>20 mm) with or without thrombosis, portal hypertension, biliary obstruction |
| Gas | At US, reverberation artifacts; at MDCT, linear branching pattern of air in the portal vein and its branches; at MR imaging, air causes suscepti-bility artifacts in the portal vein best seen on gradient-echo images with a long echo time (eg, T1-weighted in-phase images) |
| **Hepatic artery** | |
| Thrombosis | Lack of flow on color Doppler US images; lack of enhancement on MDCT and MR images; hepatic infarcts and secondary biliary com-plications such as biliary necrosis, leak, and strictures |
| Stenosis | Focal narrowing is seen at the stenosis. Doppler US demonstrates velocity changes: parvus tardus waveform (RI < 0.55, AT > 70 msec) distal to the site of stenosis, high velocity (PSV > 200 cm/sec) at the stenosis |
| Aneurysm | Focal outpouching with turbulent flow on color Doppler images, contrast agent–filled outpouching on MDCT and MR images, vascular anatomy depicted with MDCT angiography, conventional angiography used for diagnosis and therapy |
| **Biliary tree** | |
| Cholangiocarcinoma | Multiphasic MDCT or MR imaging is the modality of choice. Hilar cholangiocarcinoma is most commonly infiltrative and less common-ly mass-forming or polypoidal. MRCP demonstrates a hilar stricture with biliary enhancement. A hypo- to isoattenuating or isointense mass is characteristically seen on arterial phase and venous phase images, with progressive enhancement in the delayed phase. MR imaging has higher accuracy for determining resectability. PET/CT is used for staging. |
| Intrabiliary metastasis | Enhancing intrabiliary mass within the lumen of the CBD on MDCT and MR images; concurrent intrahepatic metastasis and history of primary malignancy (colorectal cancer is the most common) are helpful clues |
| Benign biliary stricture | Typically short-segment stricture without wall enhancement, wall thickening, or mass on MDCT and MRCP images; common causes are iatrogenic (eg, after cholecystectomy or after OLT), PSC, IgG4 sclerosing disease, and Mirizzi syndrome |
| Choledochal cyst | Segmental or diffuse CBD dilatation is seen at US, MDCT, and MRI. MDCT and MR imaging better demonstrate anatomic features and complications such as choledocholithiasis and malignant transformation. MRCP also depicts a coexistent underlying anomalous pancreaticobiliary junction. |
| **Lymphatics, nerves, and connective tissue** | |
| Lymphadenopathy | Enlarged lymph nodes (>6 mm in short-axis diameter) surround the portal vein and hepatic artery; bulky homogeneous nodes suggest low-grade lymphoma; necrotic nodes suggest metastasis, infection, and high-grade lymphoma. Reactive enlarged lymph nodes can be seen in patients with cirrhosis and indicate an immunologic response of the host to the hepatitis C virus. |
| PTLD | Characteristic ill-defined periportal soft-tissue mass, often with encasement of hilar structures with mass effect and displacement; usually hyperintense on T2-weighted images with variable enhancement |
| Schwannoma or neurilemmoma | Well-encapsulated mass with or without calcification and cystic change; heterogeneous and predominantly central enhancement |
| Neurofibroma | Unencapsulated hypoattenuating periportal sheathlike mass, often infiltrative; encases porta hepatis vessels, usually minimally enhancing |
| Sarcoma | Large mass with heterogeneous attenuation, signal intensity, and enhancement; nonspecific imaging characteristics; surgical excision required for definitive diagnosis |

Note.—AT = acceleration time, CBD = common bile duct, OLT = orthotopic liver transplant, PSC = primary sclerosing cholangitis, PSV = peak systolic velocity, RI = resistive index.

**Figure 2.** Portal vein thrombosis in a patient with liver cirrhosis. Axial contrast-enhanced CT image shows an absence of portal vein enhancement and a hypoattenuating thrombus in the lumen (arrow). Cirrhotic changes are seen in the liver, with portal hypertension in the form of ascites, splenomegaly, and extensive portosystemic collaterals.
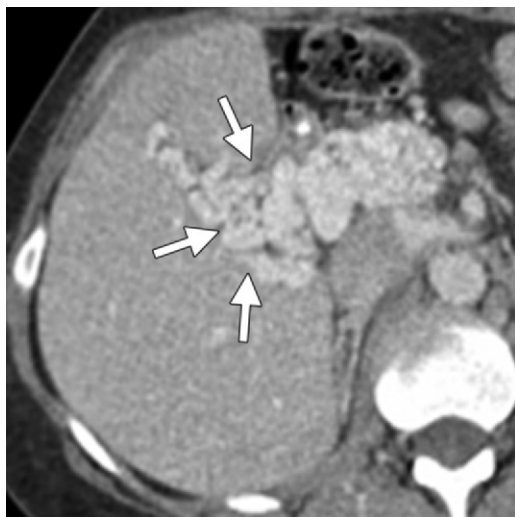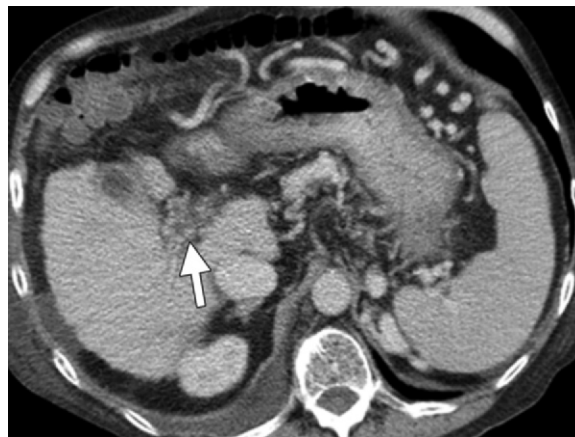


**Figure 3.** Chronic portal vein thrombosis. Axial contrast-enhanced CT image shows cavernous transformation of the main portal vein (arrows) with multiple, dilated, tortuous epicholedochal and paracholedochal collaterals at the porta hepatis that form the portoportal collateral pathway.



**Figure 4.** Portal vein thrombosis in a patient with hepatocellular carcinoma. Coronal contrast-enhanced arterial phase CT shows a hypervascular mass (black arrows) extending contiguously into the portal vein (white arrows). The portal vein is expanded and has neovascular channels, findings that suggest a malignant tumor thrombus.

thrombosis (8). Cross-sectional CT and MR imaging demonstrate the thrombus to a better advantage. Acute thrombosis is usually high attenuating on unenhanced CT images, whereas chronic thrombosis may manifest with calcifications in the expected location of the portal vein (8). Contrast-enhanced MDCT reveals a partial or complete filling defect in the portal vein and peripheral rim enhancement of the portal vein in the acute phase. Subacute and chronic thrombosis usually manifests as cavernous transformation of the portal vein, splenomegaly, and extensive portosystemic collateralization caused by extrahepatic portal hypertension. The hepatic parenchyma can show abnormal peripheral high-attenuation patches in the hepatic arterial phase or decreased enhancement in the portal venous phase (8).

Imaging also helps differentiate bland thrombosis from tumor thrombosis in patients with cirrhosis or hepatocellular carcinoma (Fig 4). Malignant portal vein thrombosis is characterized at imaging by expansile dilatation of the portal vein and intermediate to high signal intensity on T2-weighted images. In contrast, MR images of bland portal vein thrombosis usually show normal portal vein caliber and low T2-weighted signal intensity because of hemosiderin within the thrombus. A malignant thrombus shows arterial neovascularity with enhancement similar to the primary tumor and often is contiguous with the primary tumor (6) (Fig 4). Acute portal vein thrombosis is treated with anticoagulation therapy. Thrombolysis and surgical thrombectomy are performed in selected cases. Chronic portal vein thrombosis may require shunt surgery to relieve the symptoms and signs
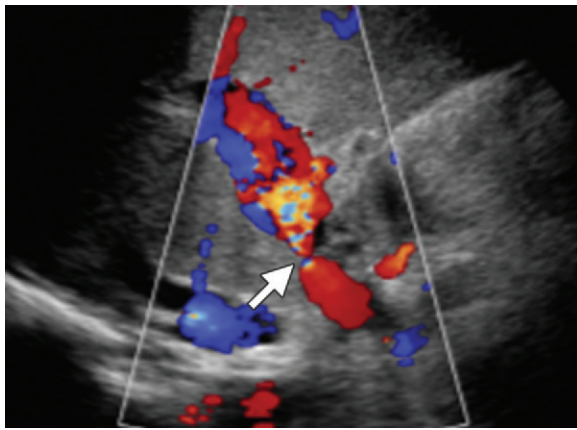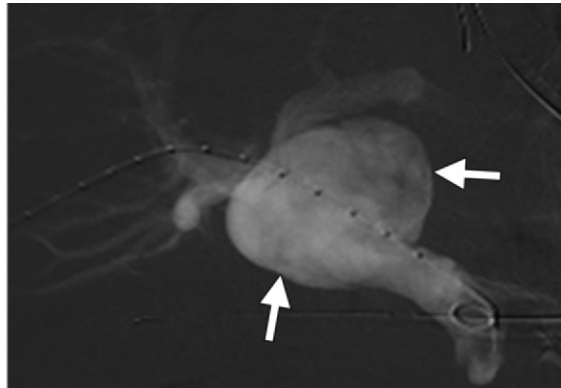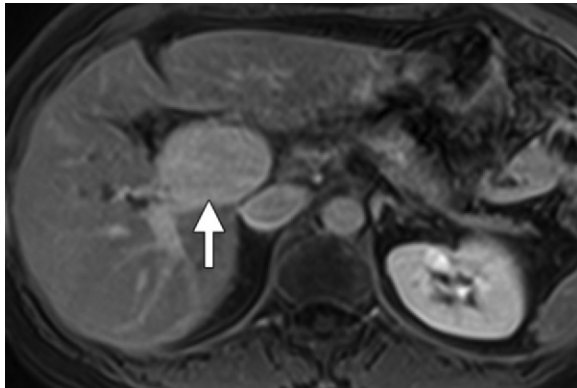
**Teaching Point**

**Figure 5.** Portal vein stenosis after liver transplantation. Transverse color Doppler US image shows focal narrowing of the portal vein (arrow) at the anastomosis with distal turbulent flow. An increased velocity gradient was seen at spectral Doppler US interrogation (not shown).



a.                                                  b.

**Figure 6.** Idiopathic aneurysm of the main portal vein. Axial gadolinium-enhanced fat-suppressed T1-weighted MR image **(a)** and transhepatic venogram **(b)** show a large portal vein aneurysm (arrows) with no evidence of underlying liver disease or portal hypertension.

of portal hypertension (4). Malignant portal vein thrombosis is treated with conformal radiation therapy, radioembolization with yttrium-90 glass microspheres, chemotherapy, hepatic resection, or a combination of these techniques (4).

*Portal Vein Stenosis.*—Portal vein stenosis is a recognized complication of liver transplantation and other surgeries that involve resection and reanastomosis of the portal vein, such as hepatic lobectomy and pancreaticoduodenectomy. Common malignant causes of portal vein stenosis include locally recurrent periampullary cancers and other neoplasms in the porta hepatis that encase the portal vein (10). Portal vein stenosis is relatively uncommon after liver transplantation; it affects an estimated 1% of transplant recipients (11) (Fig 5). Poor surgical technique, significant discrepancy between the donor and recipient vessels, excessive vessel length, hypercoagulable states, and prior portal vein surgery are predisposing factors for portal vein stenosis and thrombosis after transplantation (12). Stenosis can result in portal hypertension and massive ascites. Diagnosis is established by demonstra-

tion of a more than three- to fourfold velocity gradient across the portal vein anastomosis at spectral Doppler US, focal stenosis with or without poststenotic dilatation at gray-scale US, and focal aliasing at color Doppler US (Fig 5). Secondary portal hypertension can also be seen with an increased number and size of collaterals (13). Isolated focal anastomotic narrowing without other changes in velocity or secondary signs does not indicate portal vein stenosis. MDCT and MR imaging may also demonstrate focal narrowing of the portal vein. Symptomatic portal vein stenosis may necessitate balloon angioplasty or stent placement in the portal vein (10,12).

*Portal Vein Aneurysm.*—Aneurysms in the portal venous system account for only 3% of all venous aneurysms but are the most common type of visceral venous aneurysm (14). Their estimated prevalence is 0.6–4.3 per 1000 patients (14,15). The most common site of aneurysm is the main portal vein; just over half of cases occur within this vein (14) (Fig 6). The etiopathogenesis of portal vein aneurysms includes congenital causes such as diverticulum formation due to incomplete regression of the

distal right primitive vitelline vein, vessel wall weakness, and anomalous portal vein branching (8). Acquired causes of portal vein aneurysm include liver cirrhosis, portal hypertension, trauma, surgery, and pancreatitis. Portal vein thrombosis can give rise to aneurysms due to portal hypertension. Portal vein aneurysm usually is asymptomatic but may cause pressure symptoms if the aneurysm is large (14). Portal vein aneurysms are diagnosed at US, MDCT, and MR imaging when the portal vein diameter exceeds 20 mm (8) (Fig 6). Complications include portal hypertension, thrombosis, venous rupture, and biliary obstruction (8). Portal vein aneurysms often do not require treatment when incidentally detected but require surveillance to document growth or the development of thrombosis. Acute thrombosis may require anticoagulation therapy, percutaneous thrombolysis, or thrombectomy. Portocaval shunts and aneurysmorrhaphy are therapeutic surgical options for complicated portal vein aneurysms (16).

***Portal Vein Gas.***—Portal vein gas was traditionally recognized as an ominous sign and was thought to be associated with advanced mesenteric ischemia. With the increasing use of MDCT, portal vein gas is now detected early in cases of mesenteric ischemia, and the current reported mortality rate for mesenteric ischemia with portal vein gas ranges from 29% to 43% (17,18) (Fig 7). In addition to ischemic bowel disease, less ominous pathologic conditions such as intra-abdominal abscesses, diverticulitis, inflammatory bowel disease, and necrotizing pancreatitis, as well as iatrogenic sources such as colonoscopy and liver transplantation, can cause portal vein gas (8). Trauma, high-grade bowel obstruction, and ingestion of a caustic substance may also be associated with portal vein gas. Portal vein gas is seen on radiographs of the abdomen as linear lucent shadows in the periphery of the liver and on US images as reverberation artifacts. Portal vein gas is instantly seen at MDCT as a linear branching pattern of air in the main portal vein or its peripheral venous branches (18) (Fig 7). At MR imaging, gas in the portal vein results in susceptibility artifacts. Management requires detection of the underlying cause. Surgical intervention is necessary in cases of mesenteric ischemia, diverticulitis, and bowel obstruction. Conservative management is used for portal vein gas secondary to trauma, colonoscopy, or idiopathic causes (18).

## Diseases of the Hepatic Artery

***Common Hepatic Artery Thrombosis and Stenosis.***—Hepatic artery thrombosis is a leading cause of morbidity and mortality after orthotopic liver transplantation, with a mortality rate of



**Figure 7.**    Portal vein gas. Axial contrast-enhanced CT image shows extensive portal vein air (arrow) secondary to ischemia of the small bowel with pneumatosis (not shown). Free intraperitoneal air (arrowhead) and free intraperitoneal fluid (∗) are seen, findings that suggest bowel perforation.

about 33% in the immediate postoperative period (over 80% mortality in undiagnosed cases) (19). It is the most common vascular complication of liver transplantation. The incidence of hepatic artery thrombosis is 4%–12% in adult transplant recipients and 9%–42% in pediatric transplant recipients (11,20). *Early thrombosis* is defined as thrombosis that occurs within 1 month of transplantation, and *late thrombosis* occurs after 1 month. Risk factors for hepatic artery thrombosis include donor death due to intracerebral hemorrhage, donor age more than 50 years, previous liver transplant in the recipient, and split segmental grafts (21). Early thrombosis is caused by discrepancies in the caliber of donor and recipient arteries, increased cold ischemia time of the donor liver, and ABO blood group incompatibility (20). Late thrombosis that occurs several years after transplantation is often due to rejection and sepsis (22).

Diagnosis is made with color and pulsed Doppler US findings of lack of flow in the hepatic artery. Although Doppler US is the preferred initial imaging modality for detection, it is highly operator dependent, with sensitivity of 54%–92% and specificity of 64%–88% (23,24). False-positive imaging results can occur in patients with systemic hypotension, severe stenosis, or hepatic edema. False-negative imaging results may occur in patients with chronic thrombosis because perihepatic artery collaterals demonstrate a parvus tardus waveform and can simulate proximal hepatic artery stenosis (12,25,26). Contrast-enhanced US has been used to better characterize hepatic artery complications, with sensitivity and specificity approaching 100% in some studies (13). MDCT angiography is a
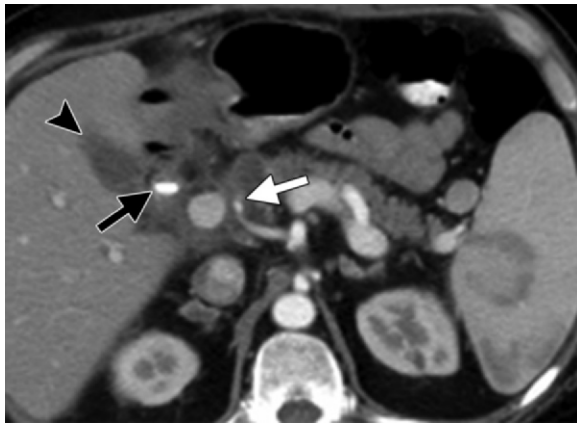
**Figure 8.** Hepatic artery thrombosis in the porta hepatis after orthotopic liver transplantation. Axial contrast-enhanced arterial phase CT image shows abrupt cutoff in the common hepatic artery (white arrow), a finding suggestive of hepatic artery thrombosis. A high-attenuating metallic clip (black arrow) and small postoperative fluid collection (arrowhead) are seen in the periportal region.
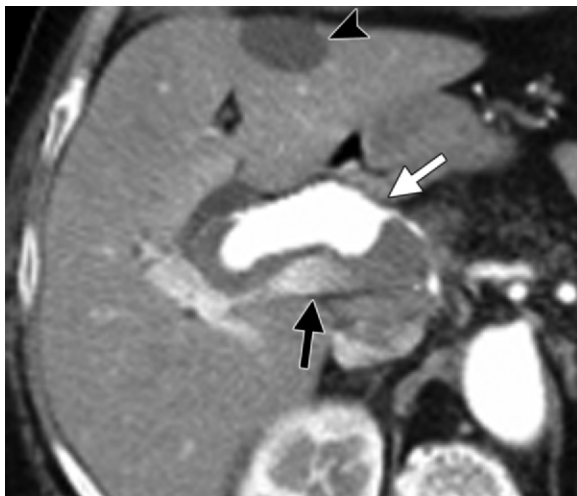


**Figure 9.** Common hepatic artery aneurysm associated with atherosclerosis. Axial contrast-enhanced arterial phase CT image shows a partially thrombosed aneurysm in the common hepatic artery (white arrow) anterior to the main portal vein (black arrow). An incidental hepatic cyst is seen (arrowhead).

reliable noninvasive modality to depict hepatic artery thrombosis. Findings at MDCT include abrupt cutoff of the hepatic artery, usually at the anastomotic site; nonenhancement of the hepatic artery; and decreased enhancement of the hepatic parenchyma due to ischemia or infarction (13) (Fig 8). MR imaging with a gadolinium-based contrast agent can show similar findings but may be technically difficult because of problems with breath-holding, especially in sick patients (13). Hepatic artery thrombosis is treated with thrombectomy or hepatic artery

reconstruction. However, most patients eventually require retransplantation, which is associated with a 30% mortality rate (13,19,26).

Hepatic artery stenosis affects 5%–13% of cases of liver transplantation and frequently occurs at the anastomosis (19,25). Complications related to stenosis include hepatic artery thrombosis, biliary ischemia, biliary strictures, sepsis, and graft loss. Diagnosis of hepatic artery stenosis is primarily established by demonstration at spectral Doppler US of a parvus tardus waveform (acceleration time > 70 msec, resistive index < 0.55) in the hepatic artery distal to the stenosis (27). At the site of narrowing, focal turbulence with a significant increase in peak systolic velocity (>200 cm/sec) can sometimes be seen (12). At MDCT and MR imaging, hepatic artery stenosis is seen as focal narrowing of the hepatic artery (28). In contrast to hepatic artery thrombosis, hepatic artery stenosis has a favorable prognosis and is managed with balloon angioplasty (12), with a primary-assisted patency of up to 87% at 6 months and 81% at 12 months (29).

***Common and Proper Hepatic Artery Aneurysm.—***
Hepatic artery aneurysm (HAA) is the second most common type of splanchnic aneurysm and accounts for up to 20% of visceral aneurysms (30). The most common site is the common hepatic artery, which is involved in up to 63% of cases (31). Common causes of HAA include atherosclerosis, fibromuscular dysplasia, collagen vascular disease, trauma (penetrating, blunt, or iatrogenic), liver transplantation, mycotic aneurysms, and tumor-related aneurysms (32) (Fig 9). Multiple aneurysms are encountered in vasculitis such as polyarteritis nodosa. Most aneurysms are incidentally detected; less than 20% of patients present with symptoms such as abdominal pain (55%) and gastrointestinal hemorrhage (46%) (32). Rupture of the aneurysm can result in hemobilia or hemoperitoneum, which is associated with a 20%–35% mortality rate (33). Communication of the aneurysm with the portal venous system can result in arterioportal fistula.

Imaging plays a major role in detecting the aneurysm and characterizing the anatomic relations that will determine its management. Color Doppler US allows real-time evaluation of the aneurysm, which will manifest as an abnormal color-filled outpouching along the course of the hepatic artery, with a characteristic "yin-yang" sign of swirling blood flow and "to and fro" waveform at the neck of the aneurysm (32,34). MDCT angiography allows evaluation of the aneurysm and the hepatic artery anatomy, including congenital variations, and assists in treatment planning (32) (Fig 10). Three-dimensional gradient-echo MR
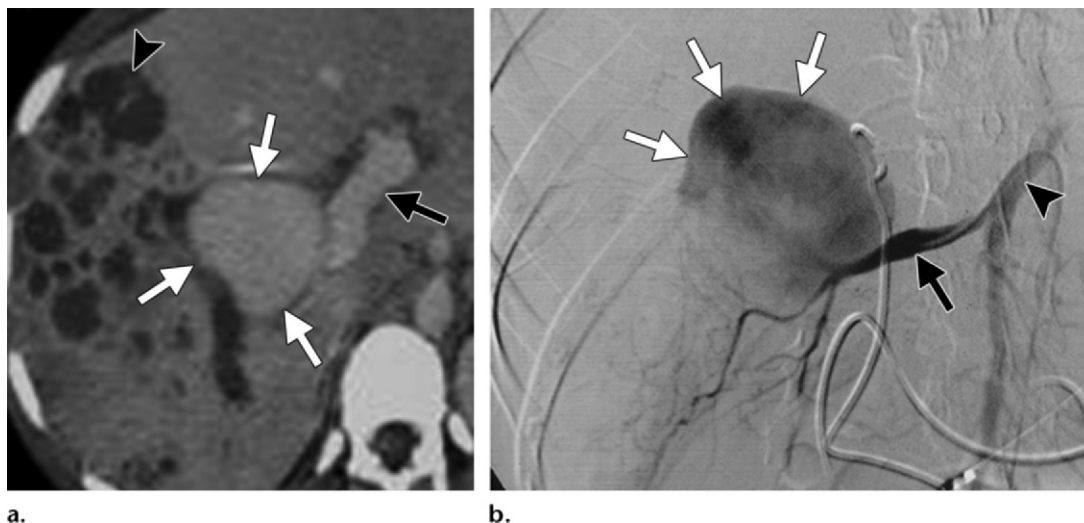
**Figure 10.** Common hepatic artery aneurysm. **(a)** Axial contrast-enhanced CT image demonstrates a contrast agent–filled outpouching (white arrows) in the porta hepatis adjacent to the portal vein (black arrow). A multiloculated abscess (arrowhead) is seen in the adjacent liver parenchyma. **(b)** Fluoroscopic image obtained at conventional catheter angiography shows a wide-necked aneurysm (white arrows) in the replaced right hepatic artery (black arrow) that arises from the superior mesenteric artery (arrowhead). The aneurysm was successfully treated with embolization.

angiography is also useful in dynamic evaluation of the arterial anatomy (35). Conventional angiography is the criterion standard for diagnosis and hemodynamic assessment because it allows real-time demonstration of the vascular bed distal and proximal to the aneurysm (32) (Fig 10).

Management of HAA depends on the location, size, and cause of the aneurysm and the regional anatomy (36). Treatment includes surgical ligation of the neck of the aneurysm or its feeding artery, embolization, or exclusion using parent-artery embolization or endovascular stenting. Interventional radiologic techniques are safe and effective and are preferred over surgery, with a success rate of 89% (37). Endovascular stenting is preferred over parent-artery embolization for treatment of proper hepatic artery aneurysm because of the risk for hepatic ischemia with embolization. Common hepatic artery embolization is associated with less risk of hepatic ischemia because of collateral flow from branches of the gastroduodenal artery (36).

## Nonvascular Diseases

### Biliary Diseases

***Hilar Cholangiocarcinoma.***—Hilar cholangiocarcinoma (Klatskin tumor) originates at the confluence of the right and left hepatic ducts in the porta hepatis and accounts for 50% of all bile duct malignancies (38). Most patients are older than 65 years at presentation. Although most cases are sporadic, predisposing conditions include primary sclerosing cholangitis, congenital biliary cystic disease, and recurrent pyogenic cholangitis (39). Presenting symptoms are nonspecific and include abdominal pain, discomfort, anorexia, weight loss, and pruritus. Jaundice is a late feature of complete biliary obstruction. Cholangitis occurs in patients with prior biliary intervention (39). Bismuth and Corlette classified hilar cholangiocarcinomas into four subtypes on the basis of the extent of ductal involvement (40). Grossly, the tumors can exhibit infiltrating (70% of tumors), intraluminal polypoidal, or mass-forming growth patterns (Figs 11, 12). Surgical resection is the only curative treatment, and its feasibility is dependent on the tumor site and the extent of biliary ductal and adjacent organ involvement (39). More than half of cases are inoperable at diagnosis because of their advanced stage. Features that suggest inoperability include invasion of the right or left hepatic duct with extension to the level of the second-order biliary radicles, atrophy of one hepatic lobe with contralateral portal vein branch or second-order biliary radicle involvement, vascular encasement or invasion of the main portal vein or main hepatic artery, and lymph node or distant metastases (38).

Imaging plays a pivotal role in determining resectability by demonstrating the extent of disease. Transabdominal sonography demonstrates intrahepatic bile duct dilatation and disruption of the confluence, with or without a polypoidal intraluminal mass and secondary lobar atrophy (Fig 12). US is less accurate for determining tumor extent and resectability. MDCT has an accu-

**Teaching Point**

11.

Figures 11, 12. (11) Infiltrating hilar cholangiocarcinoma. Axial contrast-enhanced CT image shows an infiltrative mass in the porta hepatis (arrows) causing biliary obstruction. A small amount of perihepatic ascites is also seen (arrowhead). (12) Mass-forming hilar cholangiocarcinoma. (a) Transverse US image shows a heterogeneous mass that fills the common bile duct (arrows). (b) Axial gadolinium-enhanced fat-suppressed delayed T1-weighted MR image shows heterogeneous enhancement of the mass (white arrows). Dilated intrahepatic ducts (black arrows) are seen, a finding that indicates biliary obstruction.
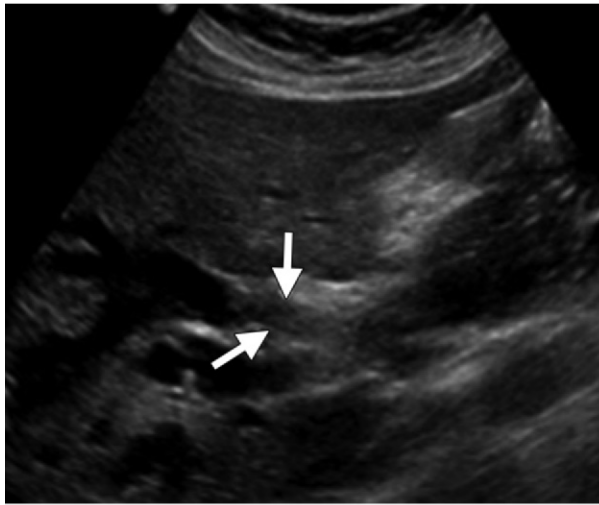


12a.
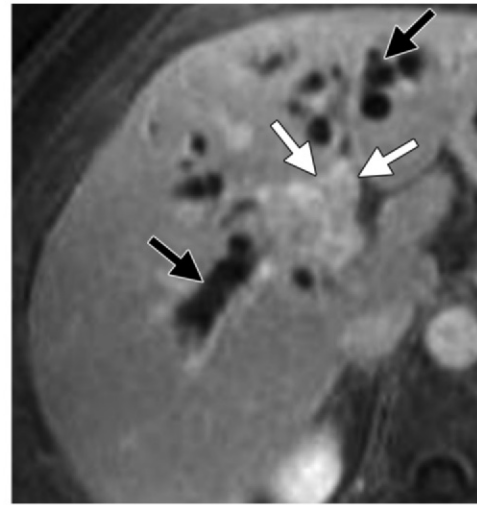


12b.

racy of 74.5%–91.7% in predicting resectability and is the noninvasive imaging modality of choice for the staging of cholangiocarcinoma (41). Multiphasic image acquisition delineates the arterial anatomy and tumor invasion at the arterial phase and portal venous encasement and hepatic parenchymal invasion at the venous phase. At MDCT, cholangiocarcinoma appears as a hypoattenuating to isoattenuating mass on arterial and venous phase images, with progressive enhancement on delayed phase images (38,41) (Fig 11).

MR imaging has the advantage of better soft-tissue contrast resolution, which allows superior depiction of tumors, especially infiltrating tumors, and better evaluation of peripheral ductal involvement. The accuracy of MR imaging for determining resectability can be as high as 93% (42). On T1-weighted MR images, hilar cholangiocarcinoma appears as a hypointense to isointense mass in the porta hepatis, with variable signal intensity on T2-weighted images (40).

On dynamic contrast-enhanced fat-suppressed T1-weighted MR images, there is heterogeneous enhancement on early images that peaks on late-phase images (Fig 12). Diffusion-weighted imaging may have added value in depicting small lesions (40). Direct endoscopic or percutaneous cholangiography is required for histopathologic diagnosis (40). The reported utility of functional imaging with FDG PET has been variable. In a study of 10 patients, Kim et al (3) reported that FDG PET is no better than conventional imaging for the assessment of hilar cholangiocarcinoma, although FDG PET may play a role in the imaging of ambiguous cases. In a study of 26 patients, Kluge et al (43) found that FDG PET has high sensitivity (92.3%) and specificity (92.9%) for identifying the primary lesion and metastases. Treatment of hilar cholangiocarcinoma is primarily surgical. Unresectable disease can be palliated with percutaneous biliary drainage or biliary stenting.

**Figure 13.** Intrabiliary metastasis from colorectal cancer. Coronal T2-weighted **(a)** and axial gadolinium-enhanced fat-suppressed T1-weighted **(b)** MR images show a heterogeneous, intermediate-signal-intensity, intrabiliary mass (white arrow in **a** and **b**) in the porta hepatis that enhanced after contrast agent administration. A synchronous parenchymal metastatic deposit also is seen (black arrows in **b**). An ERCP-guided biopsy of the mass demonstrated a metastatic deposit from colorectal cancer.



a.                                                                  b.
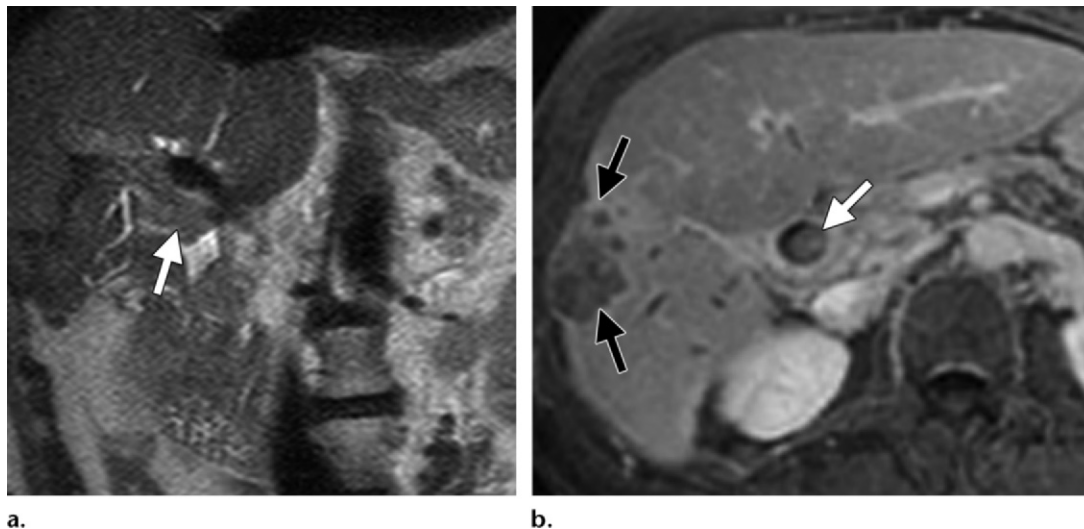
***Intrabiliary Metastases.***—Intraductal biliary metastases can mimic primary intraductal biliary neoplasms such as adenomas, papillomas, and intraductal cholangiocarcinomas (44) (Fig 13). The most common primary tumors that metastasize to the biliary tree are tumors of the lung, breast, gallbladder, colon, testis, prostate, and pancreas (44). Melanoma and lymphoma also may metastasize to the bile ducts (44). Intrabiliary invasion is seen in more than 10% of cases of resectable colorectal cancer that has metastasized to the liver (45) (Fig 13). Imaging features that favor intraductal metastasis over primary biliary malignancy include colorectal cancer as the extrabiliary malignancy and a parenchymal mass contiguous with an expansile intraductal mass (44).

***Benign Hilar Biliary Strictures.***—Many benign diseases can manifest as biliary strictures at the hepatic hilum and require a multidisciplinary approach to diagnosis and management (Fig 14). The most common cause in the Western population is iatrogenic injury related to cholecystectomy or orthotopic liver transplantation. Other causes include primary sclerosing cholangitis, IgG4-related sclerosing disease, portal biliopathy, recurrent cholangitis, and Mirizzi syndrome (46) (Fig 14). The clinical manifestation of benign strictures ranges from completely asymptomatic to severe biliary obstruction.

The incidence of biliary stricture after cholecystectomy is 0.2%–0.7% (47). Biliary strictures are the most common biliary complication of orthotopic liver transplantation. Nonanastomotic strictures often start at the hilum, occur within

6 months of transplantation, and are caused by chronic biliary ischemia secondary to hepatic artery stenosis or indolent thrombosis (46) (Fig 14). Primary sclerosing cholangitis is a chronic autoimmune inflammatory disorder that affects middle-aged men, especially those with underlying inflammatory bowel disease. Imaging demonstrates multifocal strictures of the intra- and extrahepatic biliary tree. Extrahepatic involvement may manifest as a hilar stricture (48) (Fig 14). IgG4-related sclerosing disease is an immune-mediated disorder that affects elderly men (48). Although strictures of the distal common bile duct are the most common abnormality, strictures of the intra- and extrahepatic biliary tree and perihilar strictures can be seen in up to 46% of cases (49,50) (Fig 14). *Mirizzi syndrome* refers to obstruction of the common hepatic duct due to a stone impacted in the gallbladder neck or a cystic duct and affects 0.1% of patients with gallstone disease (51). Imaging will demonstrate a stone in the gallbladder neck and proximal biliary dilatation (48) (Fig 14).

Management of benign hilar strictures revolves around maintaining the patency of the biliary tree, irrespective of the cause of the stricture. Treatment success depends on the underlying cause and the location, length, and number of strictures (48). Treatment includes endoscopy with balloon dilation and stenting or surgery (biliary-enteric anastomosis).

***Choledochal Cyst.***—Choledochal cyst, a condition characterized by cystic dilatation of the biliary tree, is a rare congenital biliary tract anomaly.

RadioGraphics

**Figure 14.**   Spectrum of benign biliary strictures. **(a)** Coronal MRCP image obtained after liver transplantation shows a hilar stricture (arrow) related to chronic ischemia. **(b)** Coronal MRCP image in a patient with primary sclerosing cholangitis shows a tight stricture (arrow) of the common hepatic duct and proximal common bile duct with intrahepatic biliary dilatation. **(c)** Coronal MRCP image in a patient with IgG4 sclerosing disease shows a stricture (arrow) of the proximal common bile duct with mild intrahepatic biliary dilatation. **(d)** Coronal ERCP image in a patient with recurrent pyogenic cholangitis shows a stricture of the common hepatic duct and proximal common bile duct (white arrow) resulting in marked intrahepatic biliary dilatation. Tiny filling defects (black arrows) in the dilated intrahepatic ducts represent intraductal calculi. **(e)** Axial T2-weighted MR image in a patient with Mirizzi syndrome shows an impacted gallstone in the cystic duct that appears as a hypointense lesion in the porta hepatis (arrow).
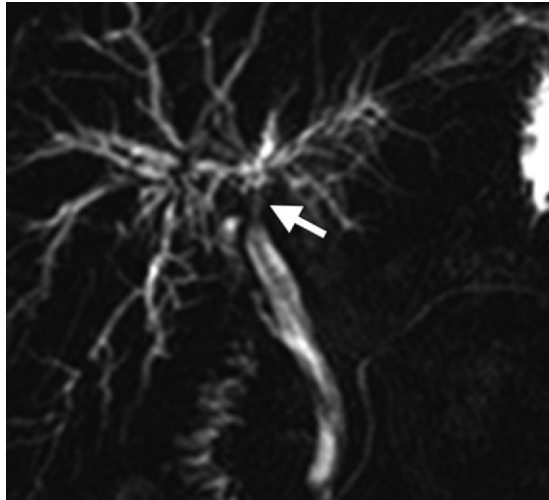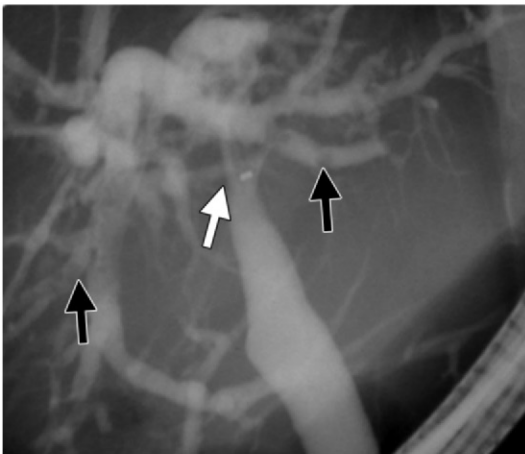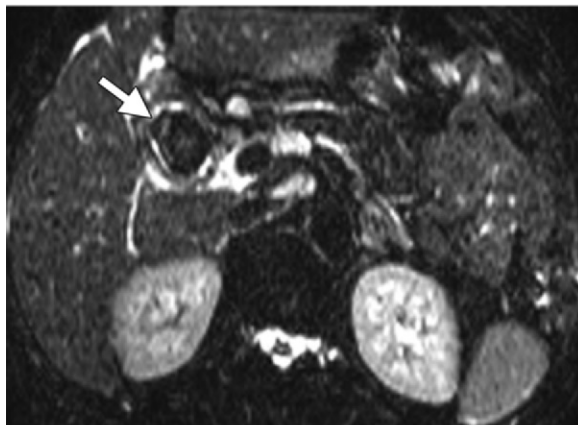


a.
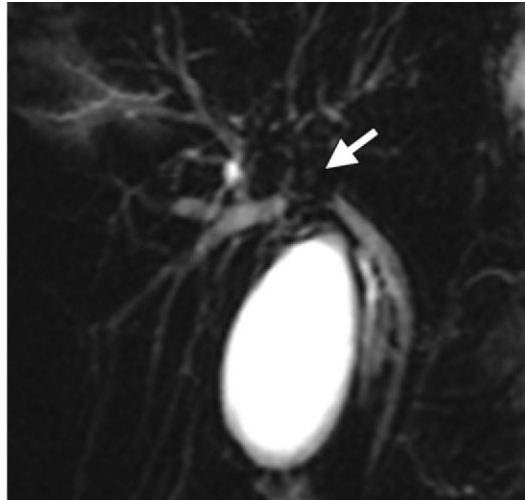
b.
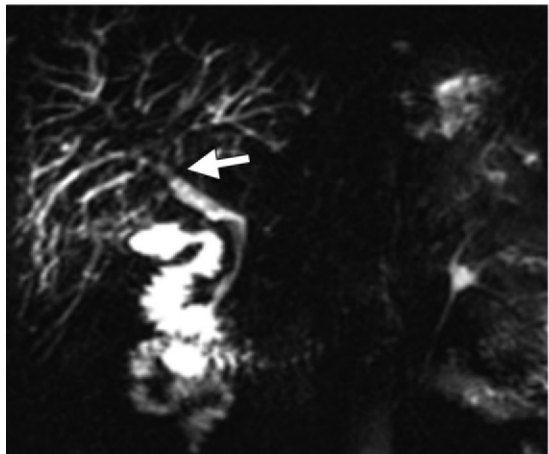
c.

d.

e.

There is a female predisposition, with a male-to-female ratio of 1:4 (52); up to 20% of patients are adults at initial treatment. Of the five types of choledochal cysts described by Todani et al (53), the type I cyst (moderate to severe dilatation of the common bile duct without intrahepatic biliary dilatation) is the most common type. Type I cysts can manifest as cystic lesions in the porta hepatis and are classified as Ia (cystic dilatation of the common bile duct), Ib (segmental dilatation of the common bile duct), or Ic (diffuse fusiform dilatation of the common bile duct) (53) (Fig 15). Clinical symptoms in adults are nonspecific; the most common presenting symptom is nonspecific abdominal pain.

US is usually the first modality that demonstrates common bile duct dilatation. MDCT and MRCP allow better evaluation of the biliary anatomy (52) (Fig 15). MRCP is particularly helpful in demonstrating an anomalous pancreaticobiliary junction with a long common channel, a finding that often coexists with choledochal cysts. Complications associated with choledochal cysts include recurrent cholangitis, cholecystitis, biliary stricture, stone formation, acute pancreatitis, and malignant degeneration (cholangiocarcinoma of the dilated duct and gallbladder cancer) (52). Treatment usually involves complete excision of the cyst with Roux-en-Y hepaticojejunostomy (53).

## Diseases of the Lymphatics, Nerves, and Connective Tissue

*Lymphadenopathy.*—The lymph nodes at the porta hepatis lie anterior and posterior to the portal vein and extend down along the hepatoduodenal ligament. Benign-appearing lymph nodes are commonly encountered in the general population but rarely exceed 6 mm in short-axis diameter (54). In a study of 156 patients, Okada et al (55) concluded that enlarged hepatoduodenal nodes seen at otherwise unremarkable US should prompt a search for underlying liver disease such as hepatitis or cirrhosis. Malignant neoplasms of the esophagus, stomach, pancreas, gallbladder, liver, biliary tree, breast, lung, and kidney can metastasize to the periportal nodes and can be associated with hepatic metastasis because the periportal nodes drain hepatic lymph (54). Lymphoma can cause bulky lymphadenopathy in the porta hepatis, especially in cases of extensive abdominal disease (Fig 16). Other causes of periportal lymphadenopathy include infections such as tuberculosis and hepatitis B and C viruses and noninfectious inflammatory conditions such as autoimmune diseases and sarcoidosis (55) (Fig 16). Bulky lymphadenopathy in the porta hepatis can result in biliary obstruction (54). Compres-
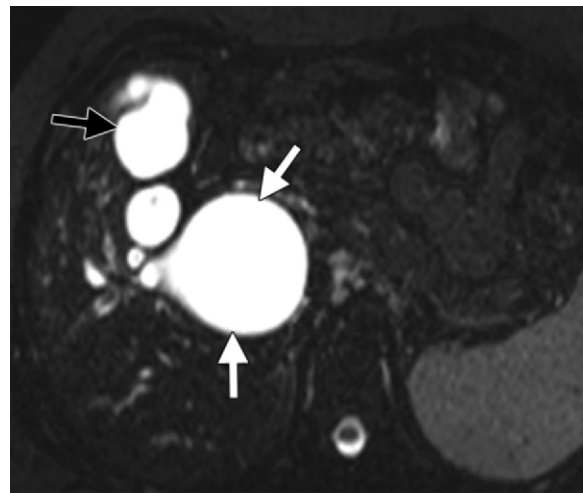


**Figure 15.** Choledochal cyst, type I. Axial fat-suppressed T2-weighted MR image shows diffuse fusiform dilatation of the common bile duct (white arrows) at the porta hepatis. Note the smooth lining of the wall with no nodularity or mass. Intrahepatic biliary dilatation was attributed to recurrent infections and stricture formation (black arrow).

sion and thrombosis of the portal vein can occur with metastatic nodes. US is a reliable and reproducible modality for demonstrating most portal and periportal lymph nodes. MDCT can help determine the extent and underlying cause of lymphadenopathy (55) (Fig 16). MRCP may be required in some cases to demonstrate associated biliary obstruction and assess the feasibility of endoscopic stenting.

*Posttransplant Lymphoproliferative Disease.*— PTLD is a unique complication of organ transplantation and is characterized by proliferation of B lymphocytes that ranges from benign proliferation to monomorphic non-Hodgkin lymphoma. The liver is the most common site of solid abdominal visceral monomorphic PTLD. Up to 45% of cases of PTLD after liver transplantation (56) and up to 40% of cases after pancreas transplantation (57) occur in the liver. After liver transplantation, PTLD and lymphomas are almost always associated with Epstein-Barr viral infection and often occur in patients who are undergoing cyclosporine therapy (26).

Hepatic involvement in PTLD can be intra- or extrahepatic. Extrahepatic involvement is frequently extranodal and appears at US and MDCT as ill-defined hypoechoic and hypoattenuating periportal heterogeneous soft tissue that encases the hilar structures. The infiltrative mass may cause narrowing of the bile duct, hepatic artery, and portal vein (58). Imaging findings of multiple parenchymal lesions or diffuse hepatic involvement with hepatomegaly support the di-

**Teaching Point**

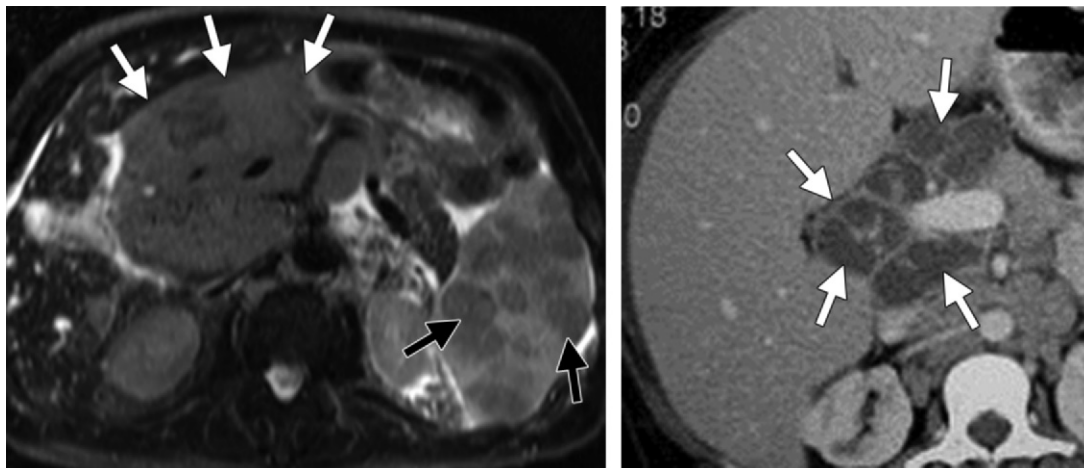**a.**                                                  **b.**

**Figure 16.**   Porta hepatis lymphadenopathy. **(a)** Axial T2-weighted MR image in a patient with non-Hodgkin lymphoma shows a large, conglomerate, intermediate-signal-intensity lymph node mass (white arrows) along the hepatoduodenal ligament that encases the main portal vein, common hepatic artery, and common bile duct and extends into the porta hepatis. Multiple splenic lymphomatous deposits are seen (black arrows). **(b)** Axial contrast-enhanced CT image in an HIV-positive patient with *Mycobacterium avium-intracellulare* infection shows extensive necrotic porta hepatis lymphadenopathy (arrows).
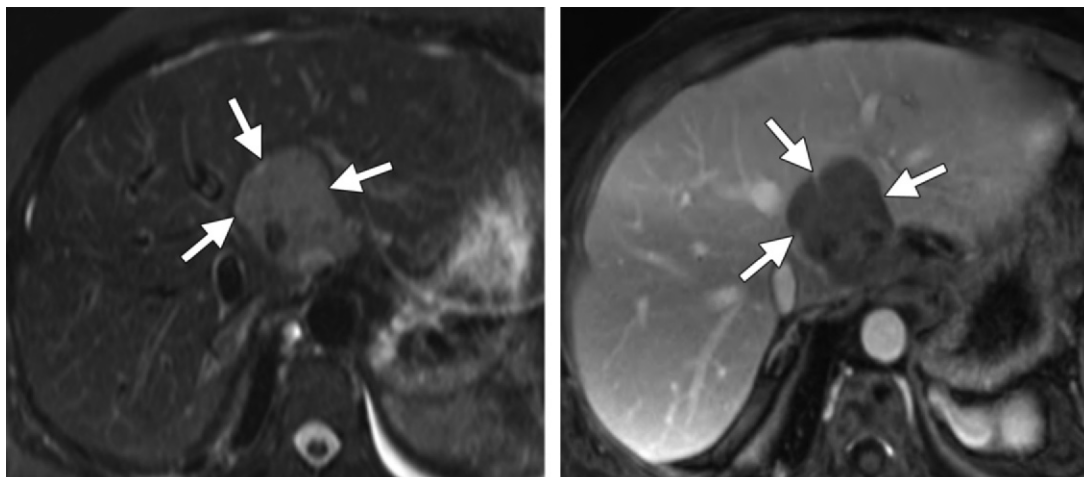


**a.**                                                  **b.**

**Figure 17.**   PTLD in a liver and kidney transplant recipient. Axial T2-weighted **(a)** and gadolinium-enhanced fat-suppressed T1-weighted **(b)** MR images show a well-defined heterogeneous mass with intermediate signal intensity in the porta hepatis (arrows) that showed mild enhancement after contrast material administration. Biopsy demonstrated monomorphic PTLD, large B-cell lymphoma type.

agnosis. At MR imaging, the lesions are hypointense on T1-weighted images and hyperintense on T2-weighted images, with variable enhancement after contrast agent administration (59) (Fig 17). Involved extrahepatic organs include the spleen, gastrointestinal tract (most commonly the small bowel), kidneys, and mesentery and adrenal glands. The differential diagnosis is post-transplant opportunistic infection. Diagnosis of PTLD requires serologic and clinical correlation. However, a periportal mass seen at imaging is a finding highly characteristic for PTLD in the appropriate clinical scenario (56).

***Neurogenic Tumors.***—Schwannoma, also known as neurilemmoma, is a benign encapsulated tumor of the nerve sheath that typically occurs in the head, neck, and extremities (60). Schwannomas of the liver are uncommon, with the majority occurring in the nerves at the porta hepatis (61). The mean patient age at diagnosis is 57.5 years, with a slight female predominance (61). Clinical symptoms are caused by compression of structures at the porta hepatis that results in obstructive jaundice. Tumors usually are slow-growing expansive masses composed of highly cellular Antoni A and loose myxoid Antoni B areas (62).

At US, schwannomas appear as complex cystic masses with hyperechoic solid areas. CT depicts them as well-encapsulated round or oval masses with calcification, cystic changes, and heterogeneous enhancement (62). At MR imaging, schwannomas are hypointense on T1-weighted images and heterogeneously hyperintense on T2-weighted images. Centrilobular delayed enhancement may be seen at dynamic imaging (62).

Hepatic neurofibroma is a rare entity often associated with extensive abdominal and retroperitoneal involvement of neurofibromatosis type 1 (63). Unlike schwannomas, neurofibromas are unencapsulated and do not contain Antoni type A and B cellular areas. Plexiform neurofibromas grow along the intrahepatic nerve fibers that accompany vessels and ducts and appear at imaging as periportal sheathlike masses (63,64). They appear as infiltrative hypoechoic masses at US and as low-attenuating masses at CT. They have low signal intensity on T1-weighted MR images and high signal intensity on T2-weighted MR images, with minimal enhancement and preservation of normal vessel distribution through the mass (63,64). Malignant transformation of neurofibromas into neurofibrosarcomas is rare (Fig 18). The differential diagnosis includes schwannoma, lymphoma, mesenchymal tumor, and atypical cystadenocarcinoma. Surgical excision is the treatment of choice for neurogenic tumors of the porta hepatis.

***Porta Hepatis Sarcomas.***—Primary sarcomas of the porta hepatis are extremely rare and can originate from biliary, vascular, or primary connective tissue (Fig 19). Biliary rhabdomyosarcomas are tumors of the pediatric population and are seen at imaging as a heterogeneous mass at the porta hepatis with biliary dilatation (65). Neurofibrosarcomas, or malignant peripheral nerve sheath tumors, of the porta hepatis are rare and are associated with neurofibromatosis type 1 (63). In a plexiform neurofibroma, inhomogeneous intense enhancement at cross-sectional imaging or hypervascular areas at angiography suggest neurofibrosarcoma (63) (Fig 18). Granulocytic sarcomas of the porta hepatis are an extremely rare cause of obstructive jaundice in patients with leukemia (66).

## Miscellaneous Diseases

***Periportal Edema.***—Periportal edema is a nonspecific imaging finding of ill-defined hypodensity at the porta hepatis or hypodensity parallel to the portal vein (67) (Fig 20). It can occur with acute hepatitis and hepatic venooclusive disease and after liver or bone marrow transplantation, over-
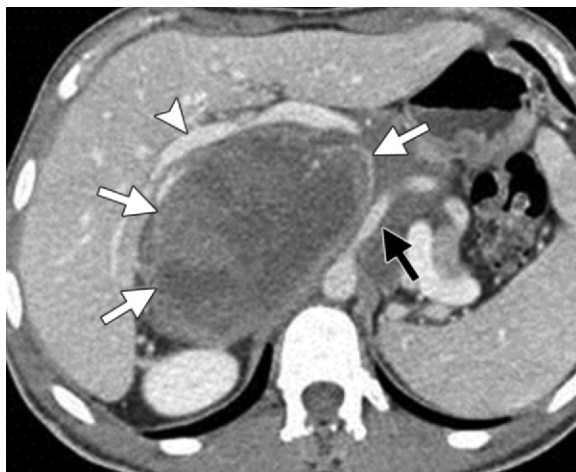


**Figure 18.** Neurofibrosarcoma of the porta hepatis. Axial contrast-enhanced CT image shows a large low-attenuation mass (white arrows) with foci of enhancement in the porta hepatis that displaces the main portal vein (arrowhead) anteriorly and the celiac trunk to the left (black arrow).
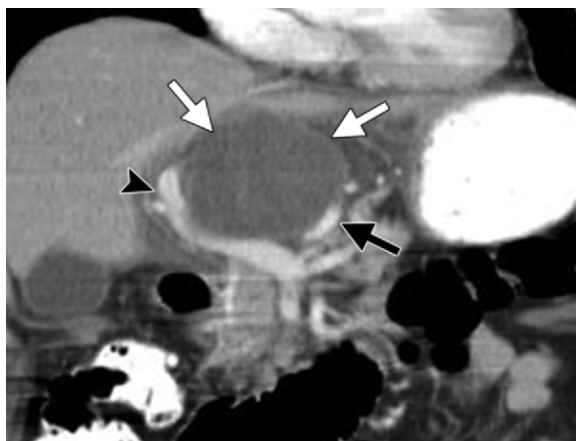


**Figure 19.** Pleomorphic epithelioid sarcoma of the hepatoduodenal ligament. Coronal contrast-enhanced CT image shows a large isolated mass (white arrows) in the porta hepatis that displaces the portal vein (arrowhead) and common hepatic artery (black arrow).

hydration, trauma, and congestive heart failure (67) (Fig 20). *Periportal halo* refers to an accumulation of lymph around the portal tract and may indicate lymphatic obstruction of the porta hepatis by a mass or lymph nodes. Persistent periportal halo in patients with lymphoma may indicate lack of response to therapy (67).
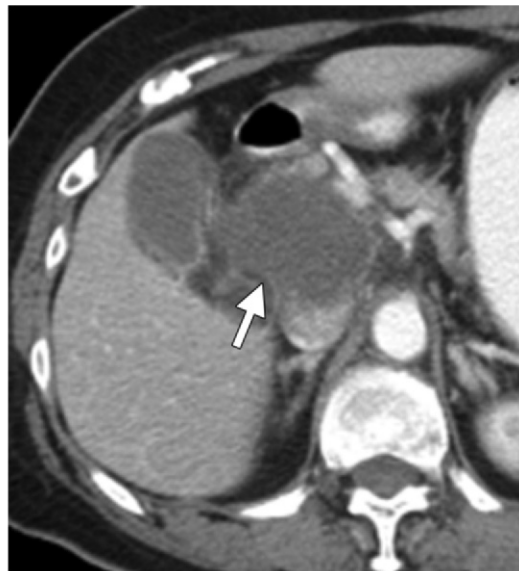
***Fluid Collections.***—Porta hepatis fluid collections such as biloma, hematoma, abscess, and seroma occur after orthotopic liver transplantation, trauma, cholecystectomy, and other biliary injuries (13) (Figs 21, 22). US is highly sensitive for detection of these collections but does not help differentiate them (12). MDCT and MR imag-

**Figure 20.**   Periportal edema. Axial contrast-enhanced CT image obtained immediately after liver transplant shows an ill-defined area of hypoattenuating soft tissue in the porta hepatis (arrows), a finding that represents periportal edema.
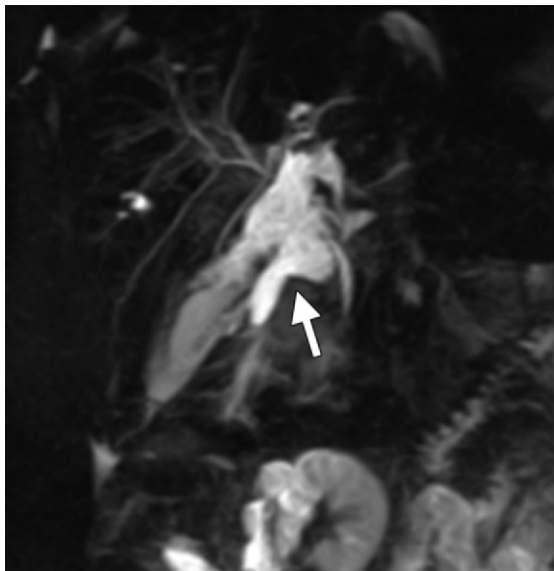


21.                                                                    22.

**Figures 21, 22.**   **(21)** Posttraumatic biloma in the porta hepatis. Coronal MRCP image obtained 2 weeks after blunt abdominal trauma shows an irregular fluid collection in the porta hepatis (arrow), a finding suspicious for bile duct injury. ERCP demonstrated a bile leak (not shown) and helped confirm occult bile duct injury. **(22)** Post-ERCP abscess in the porta hepatis. Axial contrast-enhanced CT image shows a well-defined hypoattenuating fluid collection with peripheral rim enhancement in the porta hepatis (arrow).

ing can depict the location and extent of the fluid collection, guide interventional drainage procedures, and help differentiate hematoma from biloma or seroma because of the high attenuation and different signal intensity of hematoma (68) (Fig 22). Hepatic nuclear scintigraphy can help differentiate biloma from seroma by demonstrating the site of bile leak (69).

*Trauma.*—Penetrating or blunt injuries can involve the porta hepatis and pose significant challenges in early diagnosis and management. Penetrating trauma to the porta hepatis is frequently fatal because of the involvement of vessels and frequent intraoperative exsanguination. Deep lacerations that involve the porta hepatis result in bile duct injury (70) (Fig 23). Blunt trauma to the porta hepatis has a high chance of occult biliary injury that may only be discovered later (Fig 23). Early and prompt diagnosis of vascular and biliary complications at imaging is the cornerstone of optimal successful management.

*Imaging Artifacts.*—Surgical clips from cholecystectomy, embolization, and orthotopic liver transplantation may cause artifacts at US, CT, and MR imaging (Fig 24). Beam hardening due to metallic clips can result in dark bands or streaks
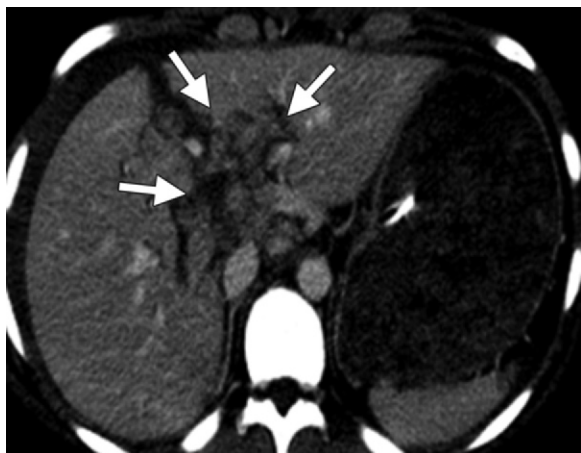
**Figure 23.** Laceration of the porta hepatis. Axial contrast-enhanced CT image obtained after blunt abdominal trauma shows multiple deep hepatic lacerations (arrows) in the porta hepatis. There was no major vascular injury. Two weeks later, the patient developed a bile leak due to occult bile duct injury.

at CT that mimic thrombosis (71). Distinctive blooming artifact at long echo time and gradient-echo sequences helps distinguish metallic artifacts from diseases such as retained biliary stones (72) (Fig 24).

***Porta Hepatis as a Pathway of Disease Spread.***—The hepatoduodenal ligament is the inferior free edge of the gastrohepatic ligament and bridges the junction of the first and second portions of the duodenum with the porta hepatis (73) (Fig 25). Peritoneal reflections in this region allow the transperitoneal spread of cancer to the porta hepatis (Fig 26). Tumors of the pancreas, duodenum, and antropyloric region of the stomach and metastases from other cancers disseminate along this route to the periportal nodes (73,74) (Fig 27).

## Conclusion

Imaging plays a crucial role in accurate diagnosis of a broad spectrum of pathologic conditions of the porta hepatis, many of which have characteristic epidemiologic, clinical, and imaging features. Knowledge of the anatomic features and diseases of the porta hepatis is essential to understand the spread of disease, diagnose underlying malignancy, and implement appropriate management.

## References

1. Weinstein JB, Heiken JP, Lee JK, et al. High resolution CT of the porta hepatis and hepatoduodenal ligament. RadioGraphics 1986;6(1):55–74.
2. Weill FS, Costaz R, Racle A, Rohmer P. Ultrasound study of adenopathies within the hepatoduodenal ligament: the "rosebud" pattern. Gastrointest Radiol 1986;11(2):142–144.



**Figure 24.** Artifact at the porta hepatis. Axial diffusion-weighted MR image of the porta hepatis shows blooming artifact (arrow) due to a metallic clip from a prior cholecystectomy.
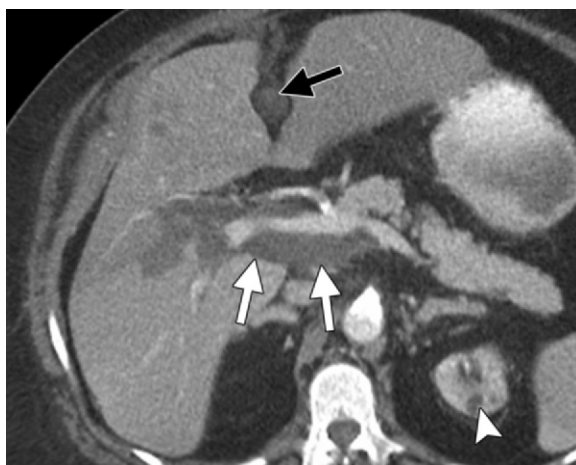


**Figure 25.** Fluid tracking along the hepatoduodenal ligament (white arrows) into the porta hepatis in a patient with a perforated duodenal ulcer. Note the fluid tracking along the falciform ligament (black arrow) and an incidental left renal cyst (arrowhead).

3. Kim YJ, Yun M, Lee WJ, Kim KS, Lee JD. Usefulness of 18F-FDG PET in intrahepatic cholangiocarcinoma. Eur J Nucl Med Mol Imaging 2003;30(11):1467–1472.
4. Chawla Y, Duseja A, Dhiman RK. Review article: the modern management of portal vein thrombosis. Aliment Pharmacol Ther 2009;30(9):881–894.
5. Amitrano L, Guardascione MA, Brancaccio V, et al. Risk factors and clinical presentation of portal vein thrombosis in patients with liver cirrhosis. J Hepatol 2004;40(5):736–741.
6. Willatt JM, Hussain HK, Adusumilli S, Marrero JA. MR imaging of hepatocellular carcinoma in the cirrhotic liver: challenges and controversies. Radiology 2008;247(2):311–330.
7. Pirisi M, Avellini C, Fabris C, et al. Portal vein thrombosis in hepatocellular carcinoma: age and sex distribution in an autopsy study. J Cancer Res Clin Oncol 1998;124(7):397–400.
8. Gallego C, Velasco M, Marcuello P, Tejedor D, De Campo L, Friera A. Congenital and acquired anomalies of the portal venous system. RadioGraphics 2002;22(1):141–159.

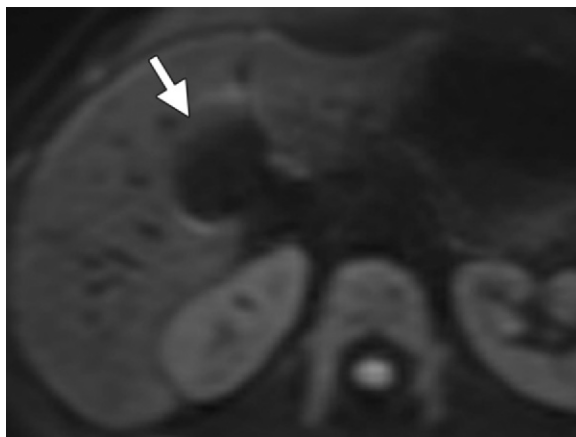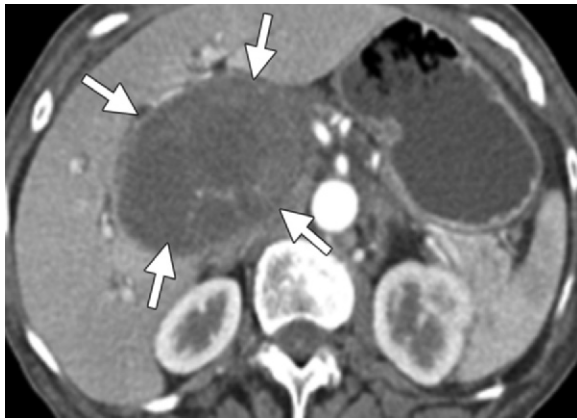**Figure 26.**   Primary peritoneal carcinoma in the porta hepatis. Axial contrast-enhanced CT image shows a large heterogeneous mass (arrows) that extends along the hepatoduodenal ligament into the porta hepatis.
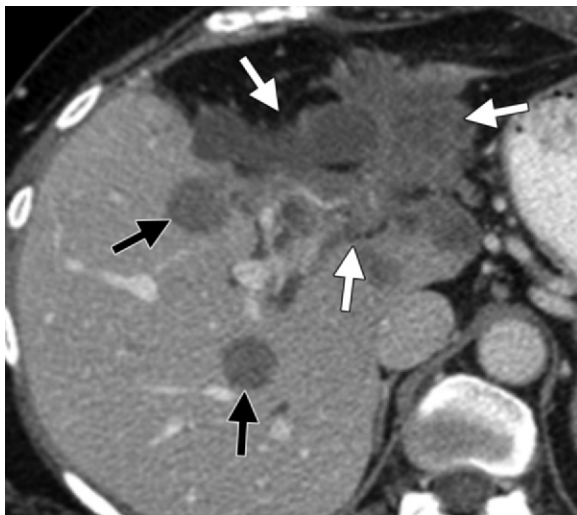


**Figure 27.**   Peritoneal metastases in the porta hepatis from primary colorectal cancer. Axial contrast-enhanced CT image shows infiltrating necrotic peritoneal metastatic deposits in the porta hepatis (white arrows) with simultaneous hepatic metastasis (black arrows).

9. Hidajat N, Stobbe H, Griesshaber V, Felix R, Schroder RJ. Imaging and radiological interventions of portal vein thrombosis. Acta Radiol 2005;46(4):336–343.
10. Kim KR, Ko GY, Sung KB, Yoon HK. Percutaneous transhepatic stent placement in the management of portal venous stenosis after curative surgery for pancreatic and biliary neoplasms. AJR Am J Roentgenol 2011; 196(4):W446–W450.
11. Wozney P, Zajko AB, Bron KM, Point S, Starzl TE. Vascular complications after liver transplantation: a 5-year experience. AJR Am J Roentgenol 1986;147(4): 657–663.
12. Crossin JD, Muradali D, Wilson SR. US of liver transplants: normal and abnormal. RadioGraphics 2003;23 (5):1093–1114.
13. Caiado AH, Blasbalg R, Marcelino AS, et al. Complications of liver transplantation: multimodality imaging approach. RadioGraphics 2007;27(5):1401–1417.
14. Koc Z, Oguzkurt L, Ulusan S. Portal venous system aneurysms: imaging, clinical findings, and a possible

new etiologic factor. AJR Am J Roentgenol 2007;189 (5):1023–1030.
15. Ohnishi K, Nakayama T, Saito M, et al. Aneurysm of the intrahepatic branch of the portal vein: report of two cases. Gastroenterology 1984;86(1):169–173.
16. Fulcher A, Turner M. Aneurysms of the portal vein and superior mesenteric vein. Abdom Imaging 1997;22(3): 287–292.
17. Muscari F, Suc B, Lagarrigue J. Hepatic portal venous gas: is it always a sign of severity and surgical emergency [in French]? Chirurgie 1999;124(1):69–72.
18. Sebastià C, Quiroga S, Espin E, Boyé R, Alvarez-Castells A, Armengol M. Portomesenteric vein gas: pathologic mechanisms, CT findings, and prognosis. RadioGraphics 2000;20(5):1213–1224, discussion 1224–1226.
19. Quiroga S, Sebastià MC, Margarit C, Castells L, Boyé R, Alvarez-Castells A. Complications of orthotopic liver transplantation: spectrum of findings with helical CT. RadioGraphics 2001;21(5):1085–1102.
20. Langnas AN, Marujo W, Stratta RJ, Wood RP, Shaw BW Jr. Vascular complications after orthotopic liver transplantation. Am J Surg 1991;161(1):76–82, discussion 82–83.
21. Stewart ZA, Locke JE, Segev DL, et al. Increased risk of graft loss from hepatic artery thrombosis after liver transplantation with older donors. Liver Transpl 2009; 15(12):1688–1695.
22. Valente JF, Alonso MH, Weber FL, Hanto DW. Late hepatic artery thrombosis in liver allograft recipients is associated with intrahepatic biliary necrosis. Transplantation 1996;61(1):61–65.
23. Horrow MM, Blumenthal BM, Reich DJ, Manzarbeitia C. Sonographic diagnosis and outcome of hepatic artery thrombosis after orthotopic liver transplantation in adults. AJR Am J Roentgenol 2007;189(2):346–351.
24. Nolten A, Sproat IA. Hepatic artery thrombosis after liver transplantation: temporal accuracy of diagnosis with duplex US and the syndrome of impending thrombosis. Radiology 1996;198(2):553–559.
25. García-Criado A, Gilabert R, Bargalló X, Brú C. Radiology in liver transplantation. Semin Ultrasound CT MR 2002;23(1):114–129.
26. Nghiem HV. Imaging of hepatic transplantation. Radiol Clin North Am 1998;36(2):429–443.
27. Vit A, De Candia A, Como G, Del Frate C, Marzio A, Bazzocchi M. Doppler evaluation of arterial complications of adult orthotopic liver transplantation. J Clin Ultrasound 2003;31(7):339–345.
28. Singh AK, Nachiappan AC, Verma HA, et al. Postoperative imaging in liver transplantation: what radiologists should know. RadioGraphics 2010;30(2):339–351.
29. Sabri SS, Saad WE, Schmitt TM, et al. Endovascular therapy for hepatic artery stenosis and thrombosis following liver transplantation. Vasc Endovascular Surg 2011;45(5):447–452.
30. Messina LM, Shanley CJ. Visceral artery aneurysms. Surg Clin North Am 1997;77(2):425–442.
31. Abbas MA, Fowl RJ, Stone WM, et al. Hepatic artery aneurysm: factors that predict complications. J Vasc Surg 2003;38(1):41–45.
32. O'Driscoll D, Olliff SP, Olliff JF. Hepatic artery aneurysm. Br J Radiol 1999;72(862):1018–1025.
33. Stanley JC, Wakefield TW, Graham LM, Whitehouse WM Jr, Zelenock GB, Lindenauer SM. Clinical importance and management of splanchnic artery aneurysms. J Vasc Surg 1986;3(5):836–840.
34. Bachar GN, Belenky A, Lubovsky L, Neuman-Levine M. Sonographic diagnosis of a giant aneurysm of the common hepatic artery. J Clin Ultrasound 2002;30(5): 300–302.
35. Liu Q, Lu JP, Wang F, et al. Visceral artery aneurysms: evaluation using 3D contrast-enhanced MR angiography. AJR Am J Roentgenol 2008;191(3):826–833.

36. Nosher JL, Chung J, Brevetti LS, Graham AM, Siegel RL. Visceral and renal artery aneurysms: a pictorial essay on endovascular therapy. RadioGraphics 2006;26 (6):1687–1704.

37. Sachdev U, Baril DT, Ellozy SH, et al. Management of aneurysms involving branches of the celiac and superior mesenteric arteries: a comparison of surgical and endovascular therapy. J Vasc Surg 2006;44(4):718–724.

38. Choi JY, Kim MJ, Lee JM, et al. Hilar cholangiocarcinoma: role of preoperative imaging with sonography, MDCT, MRI, and direct cholangiography. AJR Am J Roentgenol 2008;191(5):1448–1457.

39. Jarnagin W, Winston C. Hilar cholangiocarcinoma: diagnosis and staging. HPB (Oxford) 2005;7(4):244–251.

40. Sainani NI, Catalano OA, Holalkere NS, Zhu AX, Hahn PF, Sahani DV. Cholangiocarcinoma: current and novel imaging techniques. RadioGraphics 2008;28 (5):1263–1287.

41. Chen HW, Pan AZ, Zhen ZJ, et al. Preoperative evaluation of resectability of Klatskin tumor with 16-MDCT angiography and cholangiography. AJR Am J Roentgenol 2006;186(6):1580–1586.

42. Masselli G, Manfredi R, Vecchioli A, Gualdi G. MR imaging and MR cholangiopancreatography in the preoperative evaluation of hilar cholangiocarcinoma: correlation with surgical and pathologic findings. Eur Radiol 2008;18(10):2213–2221.

43. Kluge R, Schmidt F, Caca K, et al. Positron emission tomography with [(18)F]fluoro-2-deoxy-D-glucose for diagnosis and staging of bile duct cancer. Hepatology 2001;33(5):1029–1035.

44. Lee YJ, Kim SH, Lee JY, et al. Differential CT features of intraductal biliary metastasis and double primary intraductal polypoid cholangiocarcinoma in patients with a history of extrabiliary malignancy. AJR Am J Roentgenol 2009;193(4):1061–1069.

45. Okano K, Yamamoto J, Moriya Y, et al. Macroscopic intrabiliary growth of liver metastases from colorectal cancer. Surgery 1999;126(5):829–834.

46. Larghi A, Tringali A, Lecca PG, Giordano M, Costamagna G. Management of hilar biliary strictures. Am J Gastroenterol 2008;103(2):458–473.

47. Pitt HA, Kaufman SL, Coleman J, White RI, Cameron JL. Benign postoperative biliary strictures: operate or dilate? Ann Surg 1989;210(4):417–425, discussion 426–427.

48. Shanbhogue AK, Tirumani SH, Prasad SR, Fasih N, McInnes M. Benign biliary strictures: a current comprehensive clinical and imaging review. AJR Am J Roentgenol 2011;197(2):W295–W306.

49. Kamisawa T, Takuma K, Egawa N, Tsuruta K, Sasaki T. Autoimmune pancreatitis and IgG4-related sclerosing disease. Nat Rev Gastroenterol Hepatol 2010;7(7): 401–409.

50. Naitoh I, Nakazawa T, Ohara H, et al. Clinical significance of extrapancreatic lesions in autoimmune pancreatitis. Pancreas 2010;39(1):e1–e5.

51. Hazzan D, Golijanin D, Reissman P, Adler SN, Shiloni E. Combined endoscopic and surgical management of Mirizzi syndrome. Surg Endosc 1999;13(6):618–620.

52. Lee HK, Park SJ, Yi BH, Lee AL, Moon JH, Chang YW. Imaging features of adult choledochal cysts: a pictorial review. Korean J Radiol 2009;10(1):71–80.

53. Todani T, Watanabe Y, Toki A, Morotomi Y. Classification of congenital biliary cystic disease: special reference to type Ic and IVA cysts with primary ductal stricture. J Hepatobiliary Pancreat Surg 2003;10(5): 340–344.

54. Einstein DM, Singer AA, Chilcote WA, Desai RK. Abdominal lymphadenopathy: spectrum of CT findings. RadioGraphics 1991;11(3):457–472.

55. Okada Y, Yao YK, Yunoki M, Sugita T. Lymph nodes in the hepatoduodenal ligament: US appearances with CT and MR correlation. Clin Radiol 1996;51(3):160–166.

56. Borhani AA, Hosseinzadeh K, Almusa O, Furlan A, Nalesnik M. Imaging of posttransplantation lymphoproliferative disorder after solid organ transplantation. RadioGraphics 2009;29(4):981–1000, discussion 1000–1002.

57. Paraskevas S, Coad JE, Gruessner A, et al. Posttransplant lymphoproliferative disorder in pancreas transplantation: a single-center experience. Transplantation 2005;80(5):613–622.

58. Strouse PJ, Platt JF, Francis IR, Bree RL. Tumorous intrahepatic lymphoproliferative disorder in transplanted livers. AJR Am J Roentgenol 1996;167(5):1159–1162.

59. Pickhardt PJ, Siegel MJ. Posttransplantation lymphoproliferative disorder of the abdomen: CT evaluation in 51 patients. Radiology 1999;213(1):73–78.

60. Prévot S, Bienvenu L, Vaillant JC, de Saint-Maur PP. Benign schwannoma of the digestive tract: a clinicopathologic and immunohistochemical study of five cases, including a case of esophageal tumor. Am J Surg Pathol 1999;23(4):431–436.

61. Hayashi M, Takeshita A, Yamamoto K, Tanigawa N. Primary hepatic benign schwannoma. World J Gastrointest Surg 2012;4(3):73–78.

62. Choi H, Whitman G, Ro J, Charnsangavej C. Benign schwannoma in the porta hepatis. AJR Am J Roentgenol 2001;177(3):652.

63. Malagari K, Drakopoulos S, Brountzos E, et al. Plexiform neurofibroma of the liver: findings on MR imaging, angiography, and CT portography. AJR Am J Roentgenol 2001;176(2):493–495.

64. Gallego JC, Galindo P, Suárez I, García-Rodríguez JF. MR of hepatic plexiform neurofibroma. Clin Radiol 1998;53(5):389–390.

65. Donnelly LF, Bisset GS 3rd, Frush DP. Diagnosis please: case 2—embryonal rhabdomyosarcoma of the biliary tree. Radiology 1998;208(3):621–623.

66. Matsueda K, Yamamoto H, Doi I. An autopsy case of granulocytic sarcoma of the porta hepatis causing obstructive jaundice. J Gastroenterol 1998;33(3): 428–433.

67. Lawson TL, Thorsen MK, Erickson SJ, Perret RS, Quiroz FA, Foley WD. Periportal halo: a CT sign of liver disease. Abdom Imaging 1993;18(1):42–46.

68. Pandharipande PV, Lee VS, Morgan GR, et al. Vascular and extravascular complications of liver transplantation: comprehensive evaluation with three-dimensional contrast-enhanced volumetric MR imaging and MR cholangiopancreatography. AJR Am J Roentgenol 2001; 177(5):1101–1107.

69. Kapoor V, Baron RL, Peterson MS. Bile leaks after surgery. AJR Am J Roentgenol 2004;182(2):451–458.

70. Yoon W, Jeong YY, Kim JK, et al. CT in blunt liver trauma. RadioGraphics 2005;25(1):87–104.

71. Barrett JF, Keat N. Artifacts in CT: recognition and avoidance. RadioGraphics 2004;24(6):1679–1691.

72. Zhuo J, Gullapalli RP. AAPM/RSNA physics tutorial for residents: MR artifacts, safety, and quality control. RadioGraphics 2006;26(1):275–297.

73. Tan CH, Peungjesada S, Charnsangavej C, Bhosale P. Gastric cancer: patterns of disease spread via the perigastric ligaments shown by CT. AJR Am J Roentgenol 2010;195(2):398–404.

74. Tirkes T, Sandrasegaran K, Patel AA, et al. Peritoneal and retroperitoneal anatomy and its relevance for cross-sectional imaging. RadioGraphics 2012;32(2):437–451.

# Imaging of the Porta Hepatis: Spectrum of Disease

*Sree Harsha Tirumani, MD • Alampady Krishna Prasad Shanbhogue, MD • Raghunandan Vikram, MBBS, MRCP, FRCR • Srinivasa R. Prasad, MD • Christine O. Menias, MD*

**Page 74**

Within the porta hepatis, the common bile duct and proper hepatic artery typically are located anterior to the portal vein, with the common bile duct to the right and the proper hepatic artery to the left.

**Page 78**

Malignant portal vein thrombosis is characterized at imaging by expansile dilatation of the portal vein and intermediate to high signal intensity on T2-weighted images. In contrast, MR images of bland portal vein thrombosis usually show normal portal vein caliber and low T2-weighted signal intensity because of hemosiderin within the thrombus. A malignant thrombus shows arterial neovascularity with enhancement similar to the primary tumor and often is contiguous with the primary tumor.

**Page 81**

Diagnosis of hepatic artery stenosis is primarily established by demonstration at spectral Doppler US of a parvus tardus waveform (acceleration time > 70 msec, resistive index < 0.55) in the hepatic artery distal to the stenosis.

**Page 82**

Features that suggest inoperability include invasion of the right or left hepatic duct with extension to the level of the second-order biliary radicles, atrophy of one hepatic lobe with contralateral portal vein branch or second-order biliary radicle involvement, vascular encasement or invasion of the main portal vein or main hepatic artery, and lymph node or distant metastases.

**Page 86**

Extrahepatic involvement is frequently extranodal and appears at US and MDCT as ill-defined hypoechoic and hypoattenuating periportal heterogeneous soft tissue that encases the hilar structures.